Applied *Nanomaterials and smart Polymers,*
Online ISSN: 2981-0434
Vol. 2, No. 6

Sustainable Fatty Acid Ternary Eutectic Mixtures as Phase Change Materials: Experimental Insights and Molecular Dynamics Simulation

Iman Khanmohamadi[1], Leila Vafajoo[* 2], Mohammad Hassan Vakili[3]

[1]Department of Chemical and Polymer Engineering, ST. C., Islamic Azad University, Tehran, 1777613651, Iran. Email address: khanmohammadiiman@gmail.com
[2]Department of Chemical and Polymer Engineering, ST. C., Islamic Azad University, Tehran, 1777613651, Iran
Nanotechnology Research Centre, ST. C., Islamic Azad University, Tehran, 1584743311, Iran
E-mail address: vafajoo@azad.ac.ir, ORCID: 0000-0002-0111-446X
[3]Department of Chemical Engineering, Shahreza Branch, Islamic Azad University, Shahreza, Iran.
E-mail address: mhvakili@iaush.ac.ir

*** Corresponding Author** : Leila Vafajoo: vafajoo@azad.ac.ir

https://doi.org/10.82428/ansp.2026.1226873

Abstract
Fatty acids and their eutectic mixtures are widely recognized as desirable Phase Change Materials (PCMs) for low-to-medium temperature energy storage applications. This is due to their high energy storage density, biodegradability, sustainability, and compatibility with existing thermal systems. In the present study, the solid-liquid phase equilibrium (SLE) was investigated for ten ternary mixtures composed of Capric acid (CA), Undecylic acid (UA), Pentadecanoic acid (PA), Margaric acid (MA), and Stearic acid (SA). Both equilibrium and non-equilibrium Molecular Dynamics (MD) simulations were conducted to evaluate the thermal performance of these mixtures as PCMs. Key thermodynamic and structural properties, including temperature profiles, molecular bond energy, internal energy fluctuations, heat flux, Mean Square Displacement (MSD), hydrogen bonding interactions, and Radial Distribution Functions (RDF), were rigorously analyzed. Following the structural characterization, the melting temperatures of the ternary mixtures were predicted. The results demonstrated a strong agreement between the computational MD values and the experimental data. The comparison revealed that the developed MD simulation model predicts the melting points with high precision, showing an Average Absolute Relative Deviation (AARD) of less than 0.06%.
Keywords: Solid-Liquid Equilibrium (SLE); Phase Change Material (PCM); Melting Temperature; Energy Storage Solutions; Molecular Dynamics (MD); Environmentally Friendly Materials.

1. Introduction

In recent decades, escalating global concerns regarding energy shortages, soaring prices, and environmental degradation have necessitated the adoption of rigorous energy-saving measures and efficient energy storage solutions. Bridging the widening gap between energy production and consumption has become an imperative challenge for the scientific community [1]. Among the various technologies available, the utilization of Phase Change Materials (PCMs) has emerged as a promising approach for thermal energy storage [2-6]. PCMs offer high energy storage density and the capability to effectively store and release thermal energy during phase transitions, making them critical components in modern energy management systems.

Thermal energy storage using PCMs has garnered increasing interest as an innovative energy-saving method, finding diverse applications in fields such as construction, solar energy utilization, waste heat recovery, and waste cold management. In this context, fatty acids have risen in prominence as superior candidates for low-temperature Latent Heat Storage (LHS) applications [7], including solar drying [8] and solar desalination [9]. Compared to other available PCMs, fatty acids exhibit desirable thermodynamic and kinetic criteria, including good chemical stability, melting congruency, non-toxicity, and, most importantly, minimal volume change during phase transition. Furthermore, their high latent heat of fusion per unit mass and appropriate melting temperature range make them ideal for solar passive heating applications.

While individual fatty acids have distinct properties, their eutectic mixtures have been extensively studied to tailor melting points for specific low to medium-temperature energy storage applications. The study of fatty acid mixtures, particularly in the context of Solid-Liquid Equilibrium (SLE), relies heavily on activity models that can accurately represent the behavior of both solid and liquid phases [10-13]. Research in this domain has generally bifurcated into experimental characterization and computational modeling. Some studies have focused solely on modeling the eutectic point [14, 15], while others have aimed to predict the pre-eutectic points [16].

In the realm of experimental and thermodynamic studies, Belgodere et al. [17] established phase diagrams for ternary systems containing light fatty acids. Shilei et al. [18] investigated the thermal stability of Capric Acid (CA) and Lauric Acid (LA) eutectic mixtures. Similarly, Sari [19] and Li et al. [20] extensively studied the phase-transition properties of binary mixtures such as Margaric Acid/Stearic Acid and Lauric Acid/Pentadecylic Acid, utilizing equations like Schröeder-Van Laar for validation. Feldman et al. [21] further expanded this by investigating the heat storage capacity of fatty acid esters with alcohols.

Parallel to experimental efforts, Molecular Dynamics (MD) simulation has emerged as a powerful tool for understanding phase behavior at the atomic level, offering insights often inaccessible through experimentation alone. Kobelev et al. [22] utilized MD to simulate the liquidus curve of binary salt mixtures, while Wu et al. [23] investigated the thermal structural behavior of Lauric Acid confined within carbon nanotubes. More recently, Zhang et al. [24] and Gu et al. [25] employed MD simulations to explore the thermal properties of composite PCMs incorporating graphene and Ethylene-Vinyl Acetate (EVA). Additionally, Barani Pour et al. [26] applied MD to analyze the structural dynamics of hydrophobic eutectic solvents based on fatty acids and thymol.

Despite these advances, there remains a need for a comprehensive study that integrates experimental DSC data, thermodynamic modeling, and molecular dynamics simulation specifically for ternary fatty acid mixtures. In the present research, the authors investigate the experimental and thermodynamic aspects of solid-liquid phase equilibrium for ten distinct ternary mixtures of fatty acids. The study involves experimental investigations using

Differential Scanning Calorimetry (DSC) to examine phase transition behaviors. Furthermore, NRTL and Wilson activity models are employed with adjustable parameters derived from experimental results. To bridge the macroscopic and microscopic behaviors, Molecular Dynamics (MD) simulations are conducted for these ternary mixtures. The MD results are validated against experimental findings reported in previous work [27], focusing on estimating melting temperatures in both equilibrium and non-equilibrium phases to assess the predictive accuracy of simulation methods for sustainable energy storage materials.

2. Materials and Methods

2.1. Materials

The fatty acids employed in this study—Capric acid (CA), Undecylic acid (UA), Pentadecanoic acid (PA), Margaric acid (MA), and Stearic acid (SA)—were procured from Merck Company with a purity exceeding 98%. These materials were used in their as-received state without further purification. The thermophysical properties of pure fatty acids, critical for both experimental validation and simulation input, are summarized in Table 1.

Table 1: Thermal properties of pure fatty acids used in this study.

Material	Chemical Formula	Melting Temperature (K)	Latent Heat of Fusion (J·mol⁻¹)
Capric acid	$C_{10}H_{20}O_2$	304.8	27.79
Undecylenic acid	$C_{11}H_{20}O_2$	301.7	25.98
Pentadecanoic acid	$C_{15}H_{30}O_2$	325.7	41.53
Margaric acid	$C_{17}H_{34}O_2$	334.2	51.33
Stearic acid	$C_{18}H_{36}O_2$	342.7	61.21

2.2. Thermodynamic Modeling

To theoretically predict the melting temperatures, the thermodynamic principles of Solid-Liquid Equilibrium (SLE) were applied. The general condition for equilibrium between a solid phase and a liquid mixture is described by relating the activity of the component in the liquid phase to the heat of fusion. Based on the work of Zhang et al. [28], for an ideal eutectic mixture where the solid phase is immiscible and the liquid phase exhibits ideal behavior (Activity Coefficient $\gamma_i \approx 1$and Excess Gibbs Energy $G^{ex} \approx 0$), the simplified Schröder-Van Laar equation is utilized:

$$\ln X_i = -\frac{\Delta H_i}{R}\left(\frac{1}{T_m} - \frac{1}{T_i}\right) (1)$$

Rearranging this equation to solve for the mixture melting temperature (T_m) yields:

$$T_m = \frac{1}{\left[\frac{1}{T_i} - \frac{R\ln X_i}{\Delta H_i}\right]} (2)$$

Where:

- $T_m$is the melting temperature of the mixture (K).
- $T_i$is the melting temperature of pure component i(K).
- $X_i$is the mole fraction of component i.
- $\Delta H_i$is the latent heat of fusion of component i(J·mol⁻¹).
- $R$is the universal gas constant (8.314 J·mol⁻¹·K⁻¹).

For ternary mixtures, a pseudo-binary approach was adopted. Initially, the eutectic composition of a binary pair is calculated. This binary eutectic is then treated as a single pseudo-component,

which is subsequently mixed with the third fatty acid in varying ratios to determine the ternary eutectic point.

3. Simulation

3.1. Simulation Setup and Software

Molecular Dynamics (MD) simulations were conducted using the LAMMPS (Large-scale Atomic/Molecular Massively Parallel Simulator) software package (version 2020) [29]. Visualization and structural analysis, including Radial Distribution Function (RDF) calculations, were performed using OVITO 3.7 [30]. The primary objective was to investigate the atomic-level interactions, phase transition behaviors, and thermal properties of the ternary fatty acid mixtures.

3.2. Force Field and Potential Energy

To accurately describe the interatomic interactions within the fatty acid chains ($C-H$, $C-C$, $C=O$, and $O-H$bonds), the **OPLS-AA (Optimized Potentials for Liquid Simulations - All Atom)** force field was employed. This force field is widely recognized for its accuracy in reproducing the thermodynamic properties of organic liquids and long-chain hydrocarbons [31]. The total potential energy (E_{total}) of the system includes both bonded and non-bonded interactions:

$$E_{total} = E_{bond} + E_{angle} + E_{dihedral} + E_{vdW} + E_{Coulomb}$$

- **Bonded interactions:** Included bond stretching, angle bending, and torsional terms.
- **Non-bonded interactions:** Van der Waals forces were modeled using the Lennard-Jones (12-6) potential, while electrostatic interactions were calculated using the Coulombic law.

A cut-off radius of **10.0 Å** was applied for calculating short-range van der Waals and electrostatic interactions. Long-range electrostatic interactions were handled using the **Particle-Particle Particle-Mesh (PPPM)** solver with a precision of 10^{-4}.

3.3. Simulation Protocol

The simulation procedure comprised the following sequential steps:

1. **System Construction:** Initial atomic structures for Capric, Undecylic, Pentadecanoic, Margaric, and Stearic acids were generated. Ternary simulation boxes were created by randomly packing the fatty acid molecules according to the experimental mole fractions, ensuring an initial density close to the experimental liquid density.
2. **Energy Minimization:** To remove any steric clashes or high-energy overlaps resulting from the initial packing, the system underwent energy minimization using the Conjugate Gradient (CG) algorithm (stopping tolerance: energy 10^{-4}, force 10^{-6}).
3. **Equilibration:** The system was equilibrated in the **NVT ensemble** (constant number of particles, volume, and temperature) for **1 ns** at a temperature well above the melting point (e.g., 360 K) to ensure a homogeneous liquid mixture. The temperature was controlled using a Nose-Hoover thermostat with a damping parameter of 100 fs.
4. **Production Run (NPT):** Following equilibration, production runs were performed in the **NPT ensemble** (constant number of particles, pressure, and temperature) at 1 atm pressure. The time step was set to **1.0 fs**. The simulation extended for **10 ns** to collect data for statistical analysis.
5. **Phase Change Simulation:** To determine the melting temperature, the "Simulated Annealing" method was used. The system was cooled from the liquid phase (360 K) to

the solid phase (250 K) at a controlled cooling rate. The phase transition was identified by monitoring abrupt changes in density, internal energy, and Mean Squared Displacement (MSD).

Properties such as Radial Distribution Function (RDF), heat flux, and self-diffusion coefficients were calculated by averaging trajectories over the final 2 ns of the production run to ensure statistical reliability.

4. Results and Discussion

In this investigation, Molecular Dynamics (MD) simulation techniques were employed to analyze the molecular interactions among components within ten ternary fatty acid mixtures. The study focused on estimating temperature variations, molecular bond energy, internal energy fluctuations, thermal flux alterations, Mean Square Displacement (MSD), and Radial Distribution Functions (RDF).

The main manuscript presents the results specifically for one of the ternary mixtures: **((CA+UA)+PA)**. The findings pertaining to the remaining nine mixtures are provided in the Supplementary File.

4.1. Structural Analysis and Equilibration

Figure 1 illustrates the fundamental atomic sample structure of fatty acids employed in the initial step of the simulations.

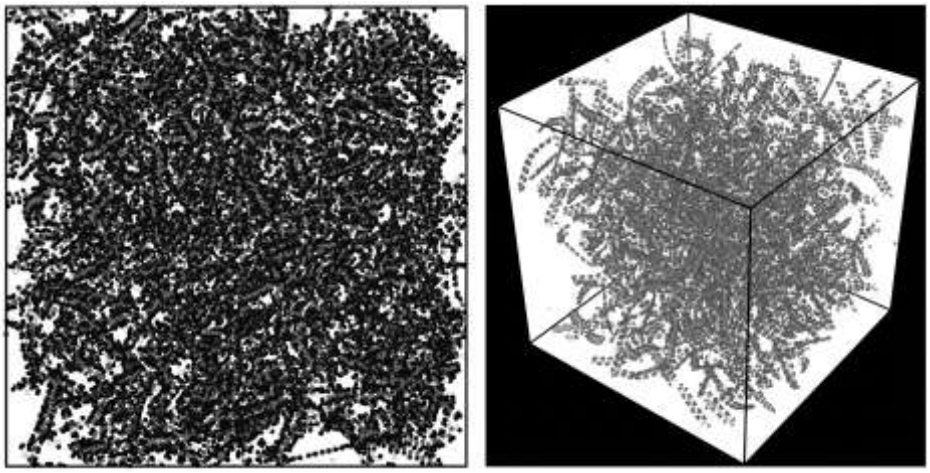

Figure 1: A sample of atomic structure arrangement in the first step of the MD simulation.

The MD simulation successfully generated the optimized 3D structures of pure Capric, Undecylic, Pentadecanoic, Margaric, and Stearic acids, as depicted in Figure 2.

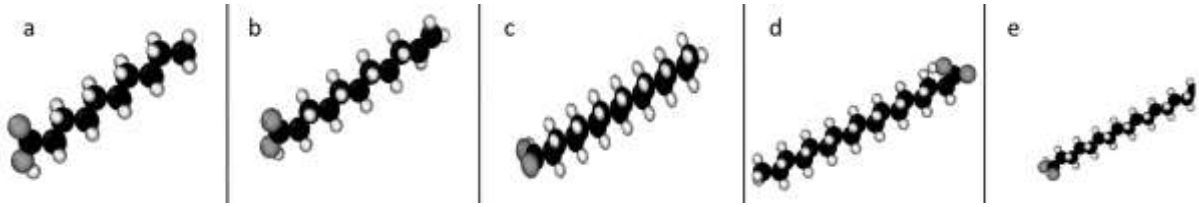

Figure 2: 3D structure of pure (a) Capric, (b) Undecylic, © Pentadecanoic, (d) Margaric, and (e) Stearic acids.

4.2. Thermal Equilibrium and Stability

Temperature variations over the simulation time for the ((CA+UA)+PA) mixture are displayed in Figure 3. The atomic structure achieved the target temperature of 300 K within a simulation time of 10 ns. This rapid stabilization indicates the accuracy of the atomic simulation setup and the appropriate adjustment of the interatomic force field (OPLS-AA). The polynomial fitting curve for the temperature data was generated using **SigmaPlot (v. 14.0)**.

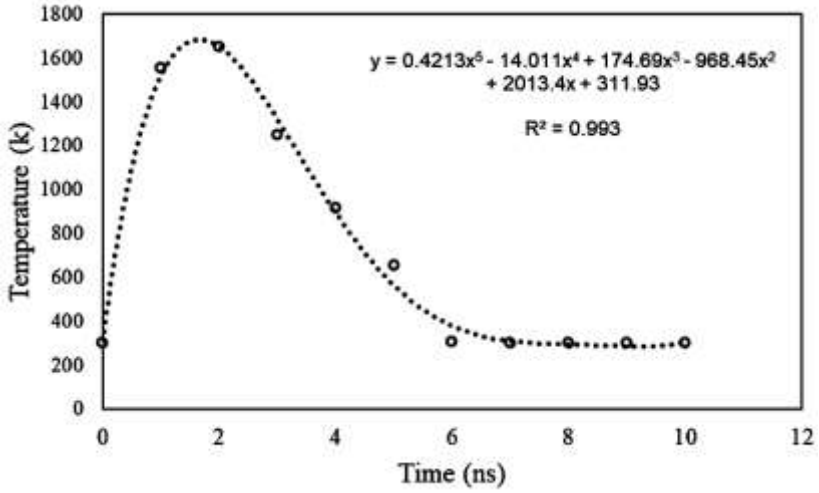

Figure 3: Temperature changes in atomic structure during the simulation.

Furthermore, the examination of the bonding energy of the simulated atomic samples demonstrates similar stability. After 10 ns, the bonding energy reached 146.21 kcal·mol^{-1}. The convergence of this value indicates a balance in the overall simulated sample. From a computational perspective, the bonding energy in the modeled structures primarily comprises bond stretching terms and angular bonding interactions.

As shown in Figure 4, the numerical value of the bonding energy tends toward a constant plateau. This stability indicates the absence of excessive repulsive forces inside the simulation box and confirms the convergence of the molecular dynamics trajectory.

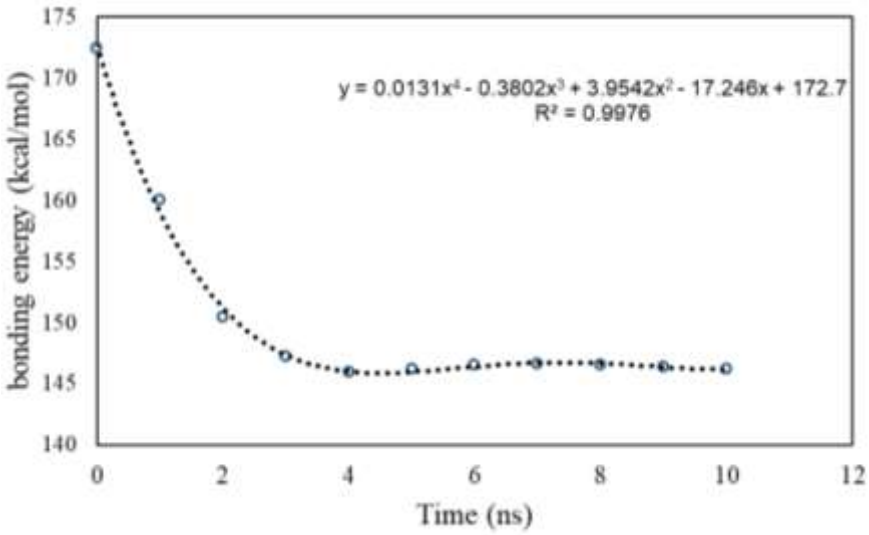

Figure 4: Bonding energy changes versus the time of the simulation process.

4.3. Internal Energy Analysis

The internal energy of the atomic structures is depicted in Figure 5. The results show that the internal energy of the overall atomic structure converged to a specific value for each sample. Based on the findings, the internal energy exhibits values ranging from 120 to 540 kcal/mol at the conclusion of the simulation.

Typically, a continuous increase in internal energy suggests heightened interatomic collisions and potential system disintegration. However, Figure 5 indicates that the internal energy remains constant as the simulation progresses. This suggests that the interatomic forces and the sample's structure were accurately implemented, and the system obeys the law of conservation of energy without atomic decay.

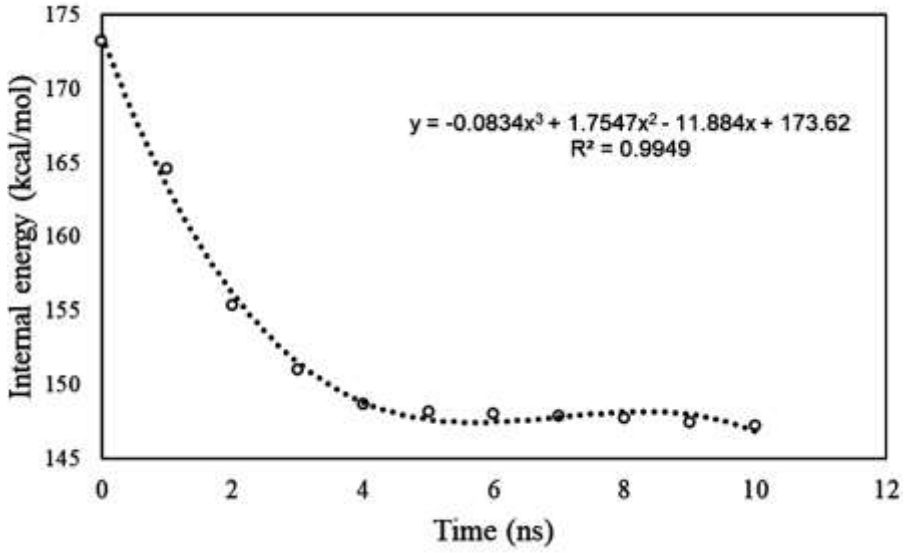

Figure 5: Internal energy changes during simulation.

4.4. Radial Distribution Function (RDF)

Figure 6 illustrates the Radial Distribution Function (RDF) specifically for the ((CA+UA)+PA) mixture. The RDF provides valuable insights into the atomic structures and interatomic distances, aiding in the characterization of the components. Mathematically, the RDF, $g(r)$, expresses the probability of finding an atom at a distance $r$from a reference atom compared to an ideal gas distribution. It is defined by the following formulation:

$$g(r) = \frac{\rho(r)}{\rho_{ideal}} (3)$$

Where $\rho(r)$is the local number density of atoms in a shell of thickness drat distance r, and $\rho_{ideal}$is the bulk number density of the system [33].

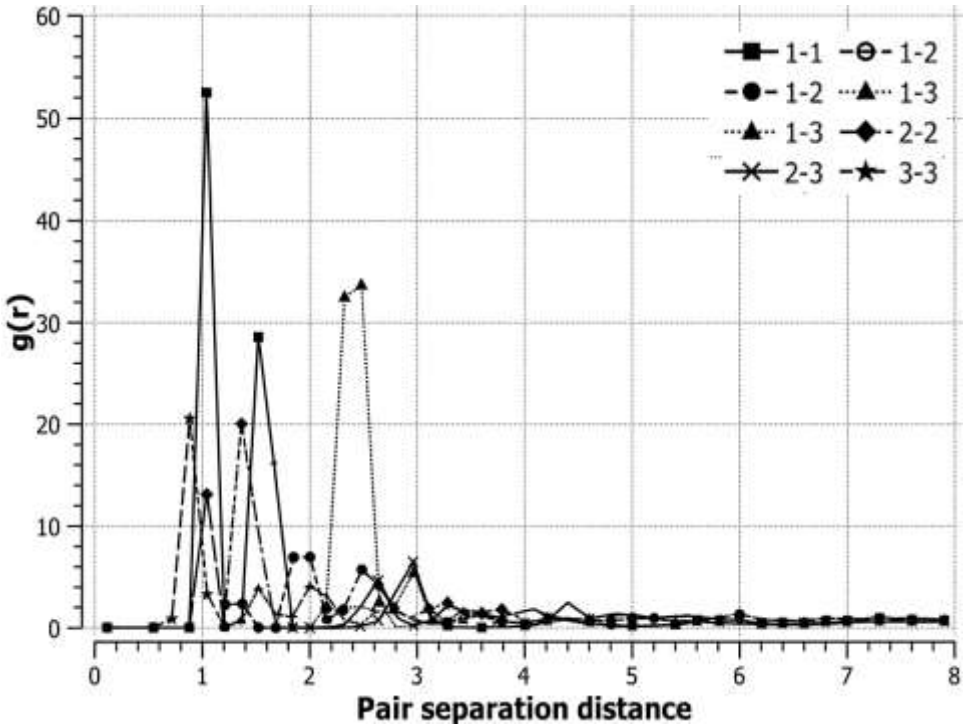

Figure 6: Radial distribution function in the simulated atomic structures.

The RDF results were calculated using **OVITO 3.7**. In the examined sample, the first peak (nearest neighbor) occurs at a distance of **0.85 Å**, and the second significant wave of atomic neighborhood appears at **2.45 Å**. In all investigated samples (presented in the Supplementary File), the nearest atomic neighbor consistently occurs at a distance of less than 1 Å, confirming the integrity of the bonded interactions within the fatty acid chains.

4.5. Heat Flux and MSD

To analyze the dynamic behavior, heat flux and Mean Square Displacement (MSD) were examined. Figure 7 depicts the heat flux for the ((CA+UA)+PA) sample.

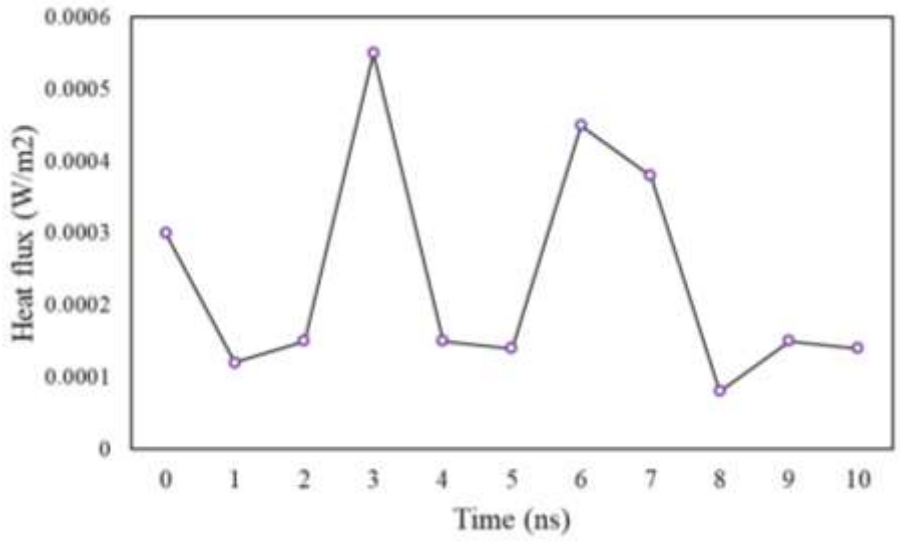

Figure 7: Heat flux changes in simulated atomic structures.

The heat flux values exhibit fluctuations attributed to inherent atomic vibrations within the simulation. However, the amplitude of these fluctuations converges, preventing excessive instability. Significant deviations in heat flux would suggest uncontrolled heat-emitting or heat-sink behaviors; the stability observed here confirms the thermodynamic consistency of the NPT ensemble.

Finally, the structural stability was assessed using the Mean Squared Displacement (MSD), shown in Figure 8.

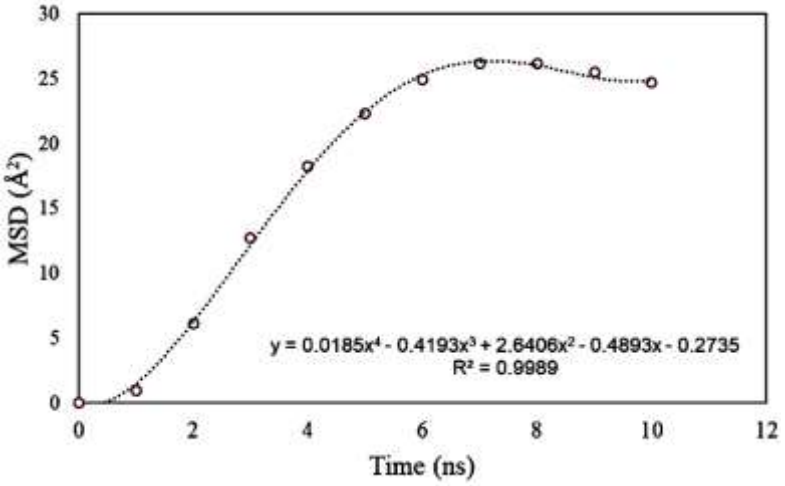

Figure 8: Variations of MSD in simulated atomic structures.

The MSD results indicate convergence to a value ranging from 25 to 45 Å² for all samples. Computationally, a stable MSD in this context (referring to the bounded motion within the simulation timeframe or phase state) reflects structural equilibrium. The convergence of this parameter represents the most desirable state in terms of stability for the modeled atomic samples.

4.6. Validation: Comparison with Experimental Data

Table 2 displays the Average Absolute Relative Deviation (AARD%) between the experimental melting points (measured in previous work [25]) and the calculated values from this MD simulation.

Table 2: AARD% of ten considered ternary mixtures correlated by the MD simulation.

Mixture System	x**(Mole Frac.)**	T_{exp}**(K)**	T_{calc}**(K)**	**AARD%**	**Mixture System**	x**(Mole Frac.)**	T_{exp}**(K)**	T_{calc}**(K)**	**AARD%**
(CA: UA) + PA	0.00	283.9	283.9	0.000	**(CA: UA) + MA**	0.00	283.9	283.9	0.000
	0.10	281.0	281.1	0.036		0.04	282.4	282.6	0.071
	0.35	308.0	307.9	0.032		0.41	315.4	315.2	0.063
	0.70	316.2	316.2	0.000		0.70	325.0	325.1	0.031
	1.00	326.5	326.3	0.061		1.00	334.2	334.4	0.060
Average				**0.026**	**Average**				**0.045**
(CA: UA) + SA	0.00	283.9	283.9	0.000	**(CA: PA) + MA**	0.00	296.5	296.5	0.000
	0.02	283.5	283.4	0.035		0.09	294.0	293.9	0.034

Mixture System	x(Mole Frac.)	T_{exp}(K)	T_{calc}(K)	AARD%	Mixture System	x(Mole Frac.)	T_{exp}(K)	T_{calc}(K)	AARD%
	0.35	324.0	323.9	0.031		0.35	318.2	318.2	0.000
	0.70	332.5	332.7	0.060		0.70	331.0	331.2	0.060
	1.00	342.8	342.8	0.000		1.00	334.5	334.5	0.000
Average				**0.025**	**Average**				**0.019**
(CA: PA) + SA	0.00	296.5	296.5	0.000	**(CA: MA) + SA**	0.00	302.0	302.0	0.000
	0.04	295.1	295.0	0.034		0.05	298.5	298.3	0.067
	0.35	328.0	327.8	0.061		0.25	326.0	325.9	0.061
	0.70	339.3	339.5	0.059		0.60	336.4	336.6	0.059
	1.00	342.1	342.1	0.000		0.85	340.8	340.8	0.000
Average				**0.031**	**Average**				**0.038**
(UA: PA) + MA	0.00	296.0	295.9	0.034	**(UA: PA) + SA**	0.00	296.0	295.9	0.034
	0.075	294.2	294.0	0.068		0.03	295.3	295.1	0.068
	0.35	313.0	312.7	0.096		0.35	321.2	321.1	0.031
	0.70	325.0	325.2	0.062		0.70	333.2	333.4	0.060
	1.00	334.5	334.5	0.000		1.00	342.1	342.1	0.000
Average				**0.052**	**Average**				**0.039**
(UA: MA) + SA	0.00	297.0	297.0	0.000	**(PA: MA) + SA**	0.00	316.2	316.2	0.000
	0.04	296.0	296.2	0.068		0.14	313.0	313.6	0.192
	0.35	321.2	321.4	0.062		0.35	325.2	325.0	0.062
	0.70	333.2	333.0	0.060		0.70	337.4	337.5	0.030
	1.00	342.1	342.1	0.000		1.00	342.1	342.1	0.000
Average				**0.038**	**Average**				**0.057**

According to the results presented in Table 2, the low AARD% values (ranging from 0.019% to 0.057%) strongly indicate the high accuracy and reliability of the molecular dynamics simulation in predicting the melting behavior of the ternary mixtures.

5. Conclusion

This study presented a comprehensive investigation into the solid-liquid phase equilibrium of ten ternary fatty acid mixtures, combining experimental measurements with advanced Molecular Dynamics (MD) simulations. The phase transition behaviors of mixtures comprising Capric acid (CA), Undecylic acid (UA), Pentadecanoic acid (PA), Margaric acid (MA), and Stearic acid (SA) were initially characterized using Differential Scanning Calorimetry (DSC). Recognizing that MD simulations have evolved into a mature technique for elucidating macromolecular structure-to-function relationships, this computational approach was employed to predict the thermophysical properties of the mixtures. The simulations rigorously estimated key properties, including temperature profiles, molecular bond energy, internal energy fluctuations, thermal flux, Mean Square Displacement (MSD), and Radial Distribution Functions (RDF).

A comparative analysis was conducted between the MD simulation results and experimental data. The findings revealed that the MD simulations predicted the melting temperatures and eutectic points with high precision. Notably, the computational results demonstrated exceptional accuracy, yielding an Average Absolute Relative Deviation (AARD) of approximately **0.04%**. This low deviation underscores the superiority of the MD approach over

some traditional thermodynamic models in capturing the complex phase behaviors of fatty acid mixtures. Consequently, this research confirms the efficacy of Molecular Dynamics as a robust and reliable tool for designing and optimizing Phase Change Materials (PCMs) for energy storage applications.

6. Supplementary Materials

Supplementary data accompanying this manuscript provides the detailed simulation results for the nine additional ternary eutectic mixtures:

1. (CA: UA) + MA
2. (CA: UA) + SA
3. (CA: PA) + MA
4. (CA: PA) + SA
5. (CA: MA) + SA
6. (UA: PA) + MA
7. (UA: PA) + SA
8. (UA: MA) + SA
9. (PA: MA) + SA

These files include comprehensive plots for temperature variations, energy profiles, and RDF analyses for each mixture. This extensive dataset serves as a valuable resource for researchers aiming to develop new PCMs and provides a foundational baseline for future studies on multi-component fatty acid systems.

References

[1] Rocha, S.A., Guirardello, R., "An approach to calculate solid–liquid phase equilibrium for binary mixtures," Fluid Phase Equilibria, 281, 12–21 (2009).
[2] Vakili-Nezhaad, G., Vatani, M., Gujarathi, A.M., "Application of Genetic Algorithm to Calculation of Three-Suffix Margules Parameters in Ternary Extraction Ionic Liquid Systems," Int. J. Therm., 17, 1-6 (2014).
[3] Kaviani, R., Naghashnejad, M., Shabgard, H., "Migration and heat transfer modeling of a neutrally buoyant melting particle in Poiseuille flow," Physics of Fluids, 35, 063327 (2023).
[4] Yu, K., Jia, M., Yang, Y., Liu, Y., "A clean strategy of concrete curing in a cold climate: Solar thermal energy storage based on phase change material," Appl. Energy, 331, 120375 (2023).
[5] Xu, F., Xu, S., & Xiong, Q., "Computational investigation of natural ventilation induced by solar chimneys: Significance of building space on thermofluid behavior," Physics of Fluids, 34, 117101 (2022).
[6] He, M., Yang, L., Zhang, Z., Yang, J., "A study on preparation and properties of carbon materials/myristic acid composite phase change thermal energy storage materials," Phase Transitions, 72, 615-633 (2019).
[7] Feldman, D., Shapiro, M. M., Banu, D., & Fuks, C. J., "Fatty acids and their mixtures as phase-change materials for thermal energy storage," Sol. Energy Mater., 18(3-4), 201-216 (1989).
{8} Kant, K., Shukla, A., & Sharma, A., "Ternary mixture of fatty acids as phase change materials for thermal energy storage applications," Energy Reports, 2, 274-279 (2016).
{9} Al-Hamadani, A. A., Shukla, S. K., & Dwivedi, A. K., "CFD application in passive building designs," In Proceedings of the National Conference on Trends and Advances in Mechanical Engineering, YMCA University of Science and Technology, Faridabad, Haryana, Vol. 114 (2012).
[10] Moattar, M.T.Z., Nasiri, S., "Phase diagrams for liquid-liquid and liquid-solid equilibrium of the ternary polyethylene glycol dimethyl ether 2000 + tri-sodium phosphate + water system at different temperatures and ambient pressure," Calphad, 34, 222-231 (2010).
[11] Razouk, R., Beaumont, O., Hay, B., "A new accurate calorimetric method for the enthalpy of fusion measurements up to 1000 °C," J. Therm. Anal. Calorim., 136, 1163–1171 (2019).
[12] Rolemberg, M.P., "Equilíbrio sólido–líquido de ácidos graxos e triglicerídios: determinação experimental e modelagem," Doctorate Thesis on Chemical Engineering, State University of Campinas (2002).
[13] Boros, L.A.D., "Modelagem matemática e termodinâmica do equilíbrio sólido–líquido de sistemas graxos," Master Thesis on Chemical Engineering, State University of Campinas (2005).
[14] Kumar, V., Sakalkale, K., & Karagadde, S., "Convection-induced bridging during alloy solidification," Physics of Fluids, 34, 053605 (2022).

[15] Huang, X., Zhu, Ch., Lin, Y., Fang, G., "Thermal properties and applications of microencapsulated PCM for thermal energy storage: A review," Appl. Therm. Eng., 147, 841-855 (2019).
[16] Slaughter, D.W., Doherty, M.F., "Calculation of solid-liquid equilibrium and crystallization paths for melt crystallization processes," Chem. Eng. Sci., 50, 1679–1694 (1995).
[17] Belgodere, J.A., Revellame, E.D., Hernandez, R., Holmes, W., Collazos, L., Bajpai, R., Zappi, M.E., "Liquid-liquid equilibria for (volatile fatty acids + water + alcohol ethoxylates): Experimental measurement of pseudo-ternary systems," J. Chem. Thermodyn., 128, 207–214 (2019).
[18] Shilei, L., Neng, Z., Guohui, F., "Eutectic mixtures of capric acid and lauric acid applied in building wallboards for heat energy storage," Energy Build., 38, 708-711 (2006).
[19] Sarı, A., "Eutectic mixtures of some fatty acids for low-temperature solar heating applications: thermal properties and thermal reliability," Appl. Therm. Eng., 25, 2100-2107 (2005).
[20] Li, M., Kao, H., Wu, Z., Tan, J., "Study on preparation and thermal property of binary fatty acid and the binary fatty acids/diatomite composite phase change materials," Appl. Energy, 88, 1606-1612 (2011).
[21] Feldman, D., Banu, D., Hawes, D., "Low chain esters of stearic acid as phase change materials for thermal energy storage in buildings," Sol. Energy Mater. Sol. Cells, 36, 311-322 (1995).
[22] Kobelev, M.A., Tatarinov, A.S., Zakiryanov, D.O., Tkachev, N.K., "Calculation of liquidus curve in phase diagram LiCl-KCl by molecular dynamics simulation," Phase Transitions, 93, 504-508 (2020).
[23] Wu, S., Jiang, W., Ma, X., Peng, D., "Molecular dynamics simulations of lauric acid confined in carbon nanotube with high thermal conductivity," Phase Transitions, 94, 436-444 (2021).
[24] Zhang, M., Wang, C., Luo, A., Liu, Z., Zhang, X., "Molecular dynamics simulation on thermophysics of paraffin/EVA/graphene nanocomposites as phase change materials," Appl. Therm. Eng., 166, 114639 (2020).
[25] Gu, Y., Jiang, L., Jin, W., Wei, Z., Liu, X., Guo, M., Chen, L., "Experimental research and molecular dynamics simulation on thermal properties of capric acid/ethylene-vinyl/graphene composite phase change materials," J. Ind. Eng. Chem., 99, 256-263 (2021).
[26] Barani Pour, S., Sardroodi, J.J., Ebrahimzadeh, A.R., "Structure and dynamics of thymol-fatty acids based deep eutectic solvent investigated by molecular dynamics simulation," Fluid Phase Equilibria, 552, 113241 (2022).
[27] Khanmohammadi, I., Vafajoo, L., Vakili, M.H., Fazaeli, R., "Evaluation of the Thermal Properties of Ternary Mixtures of Fatty Acids for Green Thermal Energy Storage Application," Phys. Chem. Res., 10, 461-471 (2022).
[28] Zhang, Y., Su, Y., & Ge, X. (1995). Prediction of the melting temperature and the fusion heat of (quasi-) eutectic PCM. *Journal of China University of Science and Technology*, *25*, 474–478.
[29] Plimpton, S. (1995). Fast parallel algorithms for short-range molecular dynamics. *Journal of Computational Physics*, *117*(1), 1–19.
[30] Stukowski, A. (2010). Visualization and analysis of atomistic simulation data with OVITO—the Open Visualization Tool. *Modelling and Simulation in Materials Science and Engineering*, *18*(1), 015012.
[31] Jorgensen, W. L., Maxwell, D. S., & Tirado-Rives, J. (1996). Development and testing of the OPLS all-atom force field on conformational energetics and properties of organic liquids. *Journal of the American Chemical Society*, *118*(45), 11225–11236.